Large-conductance Calcium-activated Anion Channel Characteristics in Neuroblastoma Cells

M. Nobile and L. Lagostena

Istituto di Cibernetica e Biofisica, C.N.R., Genova, Italy

Abstract. Large-conductance anion channel characteristics were investigated in neuroblastoma cells (N2A) by using different configurations of the patch-clamp technique. In excised patches, the channel was induced by depolarising potentials in 90% of experiments, had a conductance of 340 pS in symmetrical 135 mmol/l NaCl and exhibited the typical bell-shape activity. Neither the channel induction nor the channel activity was affected by rising the Ca^{2+} concentration on the cytopasmic side of membranes. In cell-attached configuration the maximal channel activity was shifted towards more positive potentials in comparison to that of excised patches and an increase in intracellular Ca^{2+}, obtained by extracellular application of the Ca^{2+}-ionophore A23187 in the presence of 0.2 μmol/l Ca^{2+}, induced single-channel currents in 80% of patches compared to 31% of cell-attached experiments showing channel activity in normal conditions. In turn, application of 2 μmol/l Ca^{2+} induced channel activity in 100% of patches. The reversal potential of the channel in cell-attached patches was around −10 mV as the resting potential of cells eliciting channel activity. For cells where channel activity was not detected in cell-attached mode, the resting potential was around −45 mV. Channel activity could be restored in most whole-cell recordings in the presence of 2 μmol/l or more intracellular Ca^{2+} concentrations. The Ca^{2+}-induction and the relation between channel activity and cell resting potential seem to suggest a role of the large-conductance anion channel in resting potential modulation during some basic functions of the neuroblastoma cell proliferation.

Key words: Neuroblastoma — Large-conductance anion channels — Patch-clamp — Ca^{2+} induction — Cell resting potential

Introduction

The large-conductance anion channel was the first Cl^- selective channel described in the literature at the single-channel level. The large conductance of this channel (>200 pS), the presence of multiple subconductance states, the relatively poor selectivity between anions and cations and the low probability to induce channel

Correspondence to: Mario Nobile, Istituto di Cibernetica e Biofisica, C.N.R., via De Marini 6, 16149 Genova, Italy. E-mail: nobile@icb.ge.cnr.it

activity in cell-attached configuration are characteristics that resemble those of a homogeneous family. Instead, most of the large-conductance anion channels can be classified into two groups: (1) voltage-activated anion channels with a bell-shaped dependency (Franciolini and Petris 1990; Pahapill and Schlichter 1992; Mitchell et al. 1997). Bettendorff et al. (1993) reported that thiamine derivatives modulate these anion channels. A remarkable point is that the electrophysiological properties of this large-conductance anion channel are similar to those of the voltage-dependent anion channel (VDAC) found in the outer membrane of eukaryotic mitochondria (Dermietzel et al. 1994); (2) anion channels regulated by a pathway involving endothelin (Ets) receptors, an A1 adenosine receptor, phospholipase C (PLC), diacylglycerol, protein kinase C (PKC) and G protein (Schwiebert et al. 1992, 1994; Kajita et al. 1995). The channel activity was dependent on the presence of both permeable cations and anions (Geletyuk and Kazachenko 1985; Vaca and Kunze 1992). However, despite these differences, some observations support their possible implication in volume regulation and/or cell proliferation (Falke and Misler 1989; Becq et al. 1992; Hurňák and Zachar 1994; Wu and Shrager 1994; Kajita et al. 1995; Strange et al. 1996). In this context, Mills et al. (1994) have proposed that cell swelling through a "mechanoreceptor" activates PLC via a G protein-coupled process. PLC stimulates PKC. PKC-mediated phosphorylation depolymerizes F-actin, leading to activation of a large-conductance anion channel. However, this channel exhibits properties similar to those of group 2. It has been further shown that the ionic pathways involved in cell volume regulation strongly influence the mechanisms controlling cell proliferation (Voets et al. 1995; Schlichter et al. 1996; Wonderlin and Strobl 1996; Rouzaire-Dubois and Dubois 1998; Pappas and Ritchie 1998). Moreover, calcium signalling is involved in the regulation of cell swelling and proliferation (Means 1994; Basavappa et al. 1995; Szücs et al. 1996; Nilius et al. 1997, 1998; Pedersen et al. 1998; Santella 1998). Large-conductance anion channels activated through a mechanism involving an increase in the cytoplasmic Ca^{2+} concentration have been found in nematode muscle cells (Thorn and Martin 1987; Robertson and Martin 1996), *Xenopus* oocytes (Young et al. 1984), cortical cells from rabbit kidney (Light et al., 1990), rat peritoneal mast cells (Lindau and Fernandez 1986), Swiss 3T3 fibroblasts (Kawahara and Takuwa 1991) and *Xenopus* spinal neurons (Hussy 1992). The channel in *Xenopus* spinal neurons described by Hussy (1992) was assumed to be involved in the repolarisation phase of Ca^{2+}-dependent action potentials of long duration present at early stages of neuronal differentiation. An important aspect of the physiological role of this channel was the apparently indirect type of their Ca^{2+}-dependence. Cl^- channels become only voltage dependent for long periods of time after a transient elevation of intracellular free Ca^{2+}.

In the present study, we characterise large-conductance anion channels with a bell-shaped activity in cultured rat neuroblastoma cells (N2A) by using all the patch-clamp technique configurations. A similar channel has been recently described in neuroblastoma cell lines (Falke and Misler 1989; Bettendorff et al. 1993; Forshaw et al. 1993). The high density with which these channels occur in N2A

cells and the Ca^{2+}-induction could allow one to settle some issues related to the biological role of such channels in neuronal cell lines.

Materials and Methods

Cell cultures

Rat neuroblastoma cells (N2A) were grown in MEM medium (Sigma Chemical Company, St. Louis, MO, USA) supplemented with 10% foetal calf serum and 1% L-glutamine and kept at 37°C in a 5% CO_2 incubator, as previously described (Nobile and Vercellino 1997).

Table 1. Compositions of standard extracellular (*Ext*) and intracellular (*Int*) solutions

	NaCl	$CaCl_2$	$MgCl_2$	TES	EGTA	Glucose
Ext 1	130	2.0	2	10		20
Int 1 (3 nmol/lCa^{2+})	135	0.1		10	5	20
Int 2 (3 nmol/lMCa^{2+})	40	0.1		10	5	20
Int 3 (0.2 μmol/lCa^{2+})	135	3.34		10	5	20
Int 4 (2 μmol/lCa^{2+})	135	4.7		10	5	20
Int 5 (10 μmol/lCa^{2+})	135	4.96		10	5	20

Values are mmol/l for each component. TES, N-tris(hydroxymethyl) methylaminoethanesulfonic acid; EGTA, ethylene glycol-bis(β-aminoethyl ether)-N,N,N',N'-tetraacetic acid.

Solutions

The compositions of the standard extracellular and intracellular solutions are given in Table 1. As an alternative, the NaCl salt in solutions *Ext 1* and *Int 1* was replaced with KCl; N-methyl-D-glucamine ($NMDG^+$) chloride; Na-glutamate, NaF, NaI, NaBr, Na-isethionate. The pH was adjusted to 7.3 with NaOH, KOH or $NMDG^+$, depending on the solution type, and osmolarity was set to 320 ± 5 mOsmol with mannitol. The activities of the Na^+, Ca^{2+} and K^+ channels were usually abolished by adding 0.3 μmol/l tetrodotoxin (TTX), 50 μmol/l Cd^{2+} and 10 mmol/l tetraethylammonium (TEA) to the extracellular solution. Solutions were applied by using a gravity perfusion system (≈ 1ml/min flow). Whenever external Cl^- concentration had to be changed, an agar bridge was used as the ground electrode to minimise changes in junction potential. The residual change was assessed and corrected in current-voltage relationships. In the cell-attached mode, intracellular Ca^{2+} concentration was elevated by extracellular application of 10 μg/ml of the Ca^{2+}- ionophore A23187 in the presence of 0.2 or 2 μmol/l Ca^{2+} (Table 1). A23187 was dissolved in dimethyl sulfoxide (DMSO), aliquoted, and stored frozen. Aliquots

were thawed and added directly to the bath solution before each set of experiments. The final DMSO concentration was 0.1%. All the chemicals were purchased from Sigma Chemical Co. All the experiments were carried out at room temperature (20–22 °C).

Electrophysiological measurements

Ionic currents were recorded by the patch-clamp technique in cell-attached and inside-out configurations, as in our previous studies (Nobile and Vercellino 1997; Nobile and Lagostena 1998). Borosylicate glass electrodes were pulled and calibrated to have a tip resistance of 5–10 MΩ when filled with the aforesaid solutions. Current records were filtered at 3 kHz through an 8-pole low-pass Bessel filter. Voltage stimulation and data acquisition were performed by an IBM compatible 80486 personal computer through a 12-bit interface (Axon Instruments Inc., Foster City, CA). Currents were sampled at a frequency of 100 μs per point. Fast capacitance transient compensation was performed during the experimental procedure. Current traces were analysed using pClamp (Axon Instruments Inc.) and Sigma Plot (Jandel Scientific, Erkrath, Germany) software. Single-channel currents obtained by voltage pulses 600 ms- or 30 s-long were not corrected for leakage. The analysis was performed on patches showing the activity of only one channel. Channel inactivation was examined by ensemble averages over 15 successive records obtained by 600 ms-long voltage steps applied at a frequency of 0.05 Hz. Data are given as mean values ± S.D.; Student's t test for paired data was performed and $p \leq 0.05$ was regarded as being significant.

Results

Large-conductance anion channel activity in excised patches

Excised patches of cultured rat neuroblastoma cells (N2A) displayed the activities of large-conductance channels, which were characterised by a peculiar voltage dependence. This channel type was induced within 1 to 8 min in about 90% (126/140) of patches by depolarisation. In symmetrical Cl^-, the channels were normally open at potentials close to 0 mV, but higher voltage steps, in either positive or negative directions, induced the channels to enter a voltage-dependent inactivated state (Fig. 1A). Channel activity was recovered when the membrane potential returned to 0 mV. At all potentials, the unitary current fluctuated between one predominant current amplitude and at least two sublevels that were about one third and two thirds of the main level, respectively. The permeability for Cl^- over Na^+ and K^+ was investigated in experiments performed in inside-out patches of the type shown in Fig. 1B. In symmetrical Cl^- (bath solution *Int 1*, pipette solution *Ext 1*), the conductance was 338 ± 21 pS ($n = 8$). When the internal side of the membrane was perfused in turn with 40 mmol/l NaCl (*Int 2)* or KCl, the reversal potential shifted to −17.8 ± 1.1 mV ($n = 4$) or −18.9 ± 0.5 mV ($n = 3$), respectively. The permeability ratios for Na^+ and K^+ with respect to Cl^-, calculated from the reversal

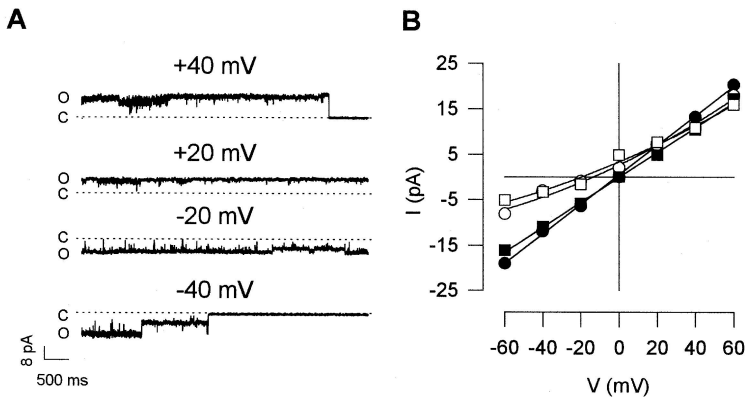

Figure 1. Large-conductance anion currents obtained from inside-out patches. A) Single-channel currents obtained from an inside-out patch (bath solution *Int 1*, pipette solution *Ext 1*). Membrane potentials related to a holding potential of 0 mV are indicated on top of each trace. The dashed lines represent zero current levels. Note the unitary current fluctuation between one predominant current amplitude and sublevels. Traces filtered at 0.5 kHz. B) Current-voltage relationships of the channel in symmetrical and asymmetrical NaCl or KCl from two different inside-out patches. The cytoplasmic sides of the patches were alternately perfused with *Int 1* (●)and *Int 2* (○) solutions or with *Int 1* (KCl salt; ■) and *Int 2* (KCl salt; □) solutions. Regression fit of current amplitudes gave a reversal potential of 0 and −17 mV for NaCl gradients and a reversal potential of 0 and −19 mV for KCl gradients.

potentials using the Goldman-Hodgkin-Katz equation, gave the following results: $P_{Cl}/P_{Na} = 4.2 \pm 0.4$, and $P_{Cl}/P_K = 4.6 \pm 0.5$. Unlike Vaca and Kunze (1992), we also observed channel activity in symmetrical NMDGCl salt. In these conditions the maximum slope conductance was 255 ± 15 pS ($n = 12$). To determine what anion permeates the channel, in twenty-six experiments Cl^- ions were replaced on the intracellular side with other halides and with organic anions such as glutamate and isethionate. On the basis of the reversal potentials, the permeability sequence was: I>Br>Cl>isethionate>F>glutamate (data not shown).

In the voltage range of about ±20 mV, long channel openings to the main level were separated by brief closed intervals of a few milliseconds. The distribution of channel open- and closed-time durations at 20 mV, determined from records that contained a single channel, was best fitted by two exponential functions (see Fig. 2A,B). Periods of rapid flickering and sublevel states, alternating with long openings with short closures, were not included in the analysis. A change of potential from 20 to −20 mV decreased the opening time constants τ_{o1} and τ_{o2} by about 30% and 50%, respectively ($p < 0.05$; $n = 3$). The closed time constants τ_{c1} and τ_{c2} were less sensitive to the potential. The fast component τ_{c1} was unaffected ($p > 0.05$; $n = 3$), whereas τ_{c2} increased by about 25% ($p < 0.05$; $n = 3$).

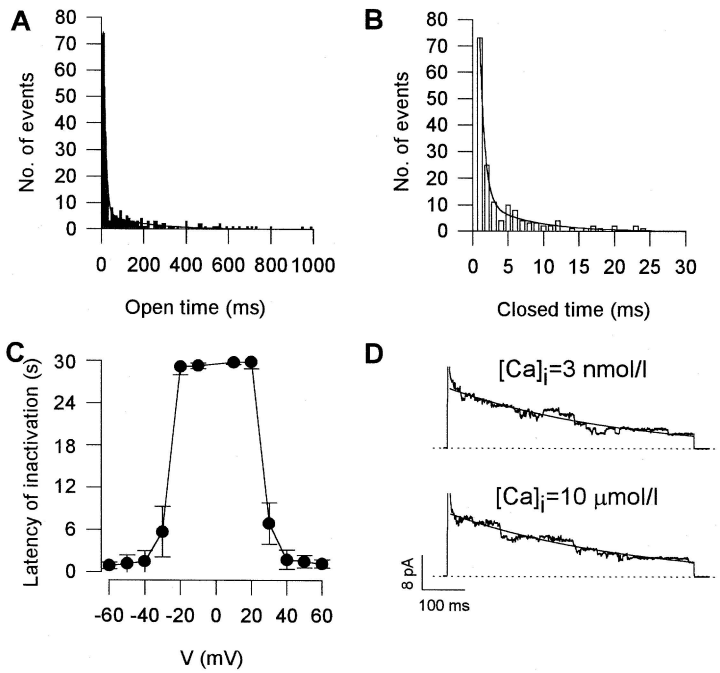

Figure 2. Kinetic characteristics and latency of inactivation of the large-conductance anion channel in inside-out patches. A, B) Open- and closed-time distributions of the channel activity from an inside-out patch held at 20 mV membrane potential. The distributions of open and closed times were fitted by the sum of two exponential functions, with $\tau_{o1} = 10.6$ ms and $\tau_{o2} = 190.1$ ms, and $\tau_{c1} = 0.7$ ms and $\tau_{c2} = 6.5$ ms, respectively. Bath solution *Int 1*, pipette solution *Ext 1*. C) Voltage dependence of the latency of inactivation of the channel. The potential producing 50% of time spent by the channel in the active state before full inactivation was about 27 mV both at negative and positive directions. Data points represent the mean values ± S.D., $n = 6$. D) Ensemble averages over sets of recordings in the presence of 3 nmol/l (solution *Int 1*) and 10 μmol/l (solution *Int 5*) intracellular Ca^{2+} concentrations. The reconstituted whole currents were given by the averages over 15 single-channel traces recorded using stimulation patterns with pulses to 50 mV, applied every 20 s, from a holding potential of 0 mV. The inactivation of the mean currents was fitted by an exponential function, and the time constants were 408 and 416 ms. The straight lines represent the zero-current level.

Figure 2C shows the time spent by the channel in a conducting state before inactivation occurred at varying voltage steps 30 s-long. This latency of inactivation *vs* voltage relationship indicates that the potential at which the channel spent 50% of the time to full inactivation was about 27 mV both at negative and positive directions. Elevation of intracellular Ca^{2+} neither induced single-channel currents in inside-out patches that did not elicit channel activity nor affected the kinetics

of channels activated by depolarising potentials. Figure 2D shows typical current relaxations in the presence of 3 nmol/l and 10 μmol/l intracellular Ca^{2+} concentrations. The reconstituted whole currents displayed were given by the averages over 15 single-channel traces recorded by using stimulation patterns with pulses to 50 mV (applied every 20 s) from a holding potential of 0 mV. The inactivations of the mean current were fitted by an exponential function, and the time constants were 410 ±10 ms and 418 ± 12 ms, respectively ($p > 0.05$; n=3). The Cl^- channel blockers, 4,4'-diisothiocyano-2,2'-disulfonic acid stilbene (DIDS) and Zn^{2+} were tested. Addition of 100 μmol/l DIDS to the extracellular solution in outside-out experiments completely blocked active channels in about 1 min. Channel activity recovered after 5-min washing with a standard solution. Zn^{2+} at 1 mmol/l concentration added to the cytoplasmic face in inside-out patches blocked the channels within tens of seconds, and the block was quickly reversed (≈1 min) upon washing Zn^{2+} from the bath (data not shown).

Large-conductance anion channel activity in cell-attached recordings

Figure 3A,B shows unitary current traces and the current *vs* voltage relationship (I–V) for a cell-attached patch in the presence of the same solution (*Ext 1)* in the bath and the pipette. The regression fit of current amplitudes gave a maximum slope conductance of 290 ± 10 pS ($n = 8$). Cl^- channel activity was detected in 43/139 (31%) patches after application of depolarising potentials; latencies from 0 to 4 min were observed. In cell-attached patches as in excised patches the unitary channel current fluctuated between one predominant current amplitude and sublevels, and periods of rapid flickering alternating with long openings with short closures are observed. The cell resting potential, immediately recorded under current-clamp conditions in cells with elicited channel activity in cell-attached mode, was −10.7 ± 8.2 mV ($n = 17$). Consequently, the holding potential was imposed on this resting potential. The single channel current reverted to potentials close to 0 mV (−1 ± 2 mV; $n = 24$) relative to rest. In thirty-two experiments, in which channel activity in the cell-attached mode was not detected, the whole-cell configuration showed that the cell resting potential was −45.8 ± 14.1 mV. No correlation with the cell cycle was examined during the investigation period.

Elevation of intracellular Ca^{2+} by extracellular application, for 10 min, of 10 μg/ml of the Ca^{2+}-ionophore A23187 in the presence of 0.2 μmol/l Ca^{2+} induced single-channel currents in 80% ($n = 10$) of cell-attached patches. Application of the Ca^{2+}-ionophore A23187 and 2 μmol/l Ca^{2+} induced single-channel currents in 100% ($n = 10$) of cell-attached patches immediately after the seal formation. A treatment for up to 10 min with A23187 in the absence of Ca^{2+} did not elicit any channel activity in patches containing channels, as revealed by addition of Ca^{2+} to the extracellular solution ($n = 4$). Figure 3C,D shows unitary current traces and the I–V relationship for a cell-attached patch after treatment with A23187 in the presence of 0.2 μmol/l Ca^{2+} in the bath (bath solution *Int* 3, pipette solution *Ext 1*). In cells treated with the Ca^{2+}-ionophore, the channel showed a flickering behaviour due to frequent transitions between the highest opening level and the

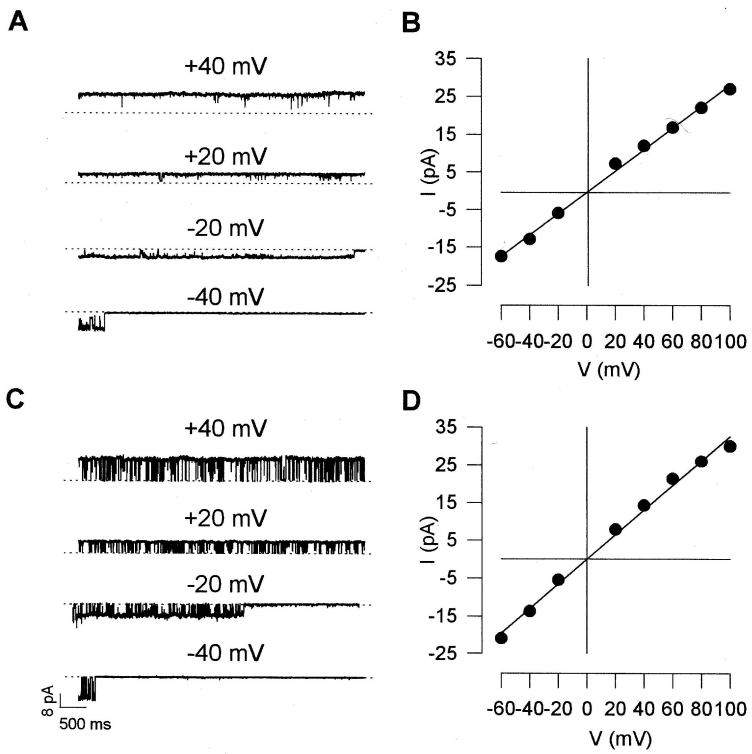

Figure 3. Large-conductance anion currents obtained in cell-attached patches. A) Single-channel traces obtained from a cell-attached patch in standard conditions (bath solution *Ext 1*, pipette solution *Ext 1*). Membrane potentials related to resting potential of cells are indicated on top of each trace. B) Current-voltage relationship for the channel in A. Regression fit of current amplitudes gave a slope conductance of 298 pS and a reversal potential of 0 mV relative to rest. C) Single-channel traces obtained from a cell-attached patch after treatment with A23187 in the presence of 0.2 μmol/l external Ca^{2+} (bath solution *Int 3*, pipette solution *Ext 1*). D) Current-voltage relationship for the channel in C. Regression fit of current amplitudes gave a slope conductance of 350 pS and a reversal potential of -1.4 mV relative to rest. Note the different single-channel kinetic behaviours in the above-indicated conditions.

baseline. Regression fit of current amplitudes gave a slope conductance of 310±15 pS and a reversal potential of 0 ± 2 mV ($n = 5$). Double exponential functions were necessary to fit open- and closed-time durations at 20 mV in normal cell-attached patches, whereas, in experiments performed in the presence of the Ca^{2+}-ionophore, the histograms were fitted by single exponential functions (Fig. 4A,B,D,E). The fast and slow components of the open and closed distributions in conventional cell-attached patches were of the same order of magnitude as those in excised patches, with τ_{o1} ranging between 10 and 22 ms, τ_{o2} between 130 and 200 ms, τ_{c1} equal

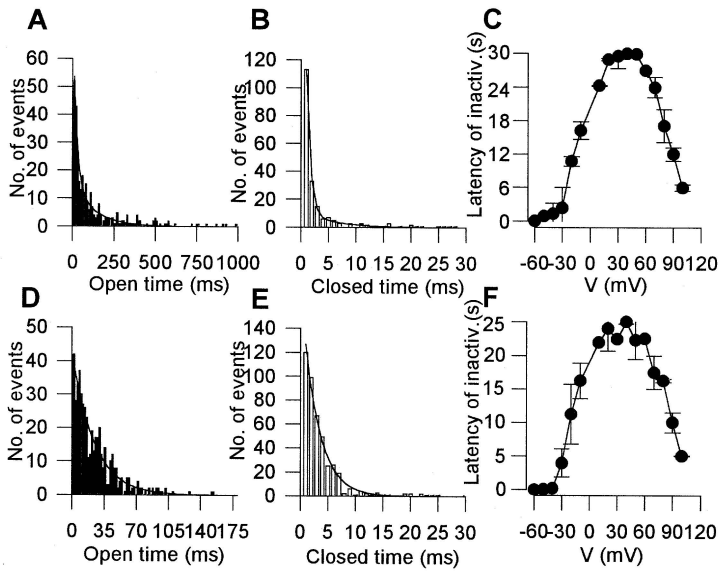

Figure 4. Kinetic characteristics and latency of inactivation of the large-conductance anion channel in cell-attached patches. A, B) Open- and closed-time distributions of the channel for a cell-attached patch held at 20 mV. The distributions of open- and closed-times were fitted by the sum of two exponential functions, with $\tau_{o1} = 21.1$ ms and $\tau_{o2} = 135.3$ ms, and $\tau_{c1} = 0.7$ ms and $\tau_{c2} = 5.8$ ms, respectively. Bath solution *Ext 1*, pipette solution *Ext 1*. C) Latency of inactivation of the channel in cell-attached patches at varying potentials ($n = 8$). Time spent by the channel in the conducting state before inactivation occurring at different potentials. The voltage-dependence was quite different from that in excised patches. D, E) Open- and closed-time distributions of the anion channel for a cell-attached patch held at 20 mV after treatment with A23187 in the presence of 0.2 μmol/l external Ca^{2+}. The distributions of open- and closed-times were fitted by a single exponential function, with $\tau_o = 24.1$ ms and $\tau_c = 3.1$ ms. Bath solution *Int 3*, pipette solution *Ext 1*. F) Latency of inactivation of the channel in cell-attached patches after treatment with A23187 ($n = 7$). The potential producing 50% of time spent by the channel in the active state before full inactivation was about -15 mV at negative potentials and 85 mV at positive potentials in both cell-attached patches and A23187-treated cell-attached patches.

to 0.7 ms in both cases, and τ_{c2} between 5 and 8 ms ($n = 5$). The open and closed distributions fitted by a single exponential gave a τ_o value of 20 ± 5 ms and a τ_c value of 2.5 ± 0.6 ms ($n = 4$). Cell-attached patches showed a less pronounced voltage-dependence of the channel latency of inactivation and the maximal channel activity shifted towards more positive potentials in comparison to that of excised patches. In Fig. 4C,F, the latency of inactivation *vs* voltage relationships obtained in cell-attached patches and in A23187-treated cell-attached patches indicates that the potential which the channel spent 50% of the time to full inactivation was about

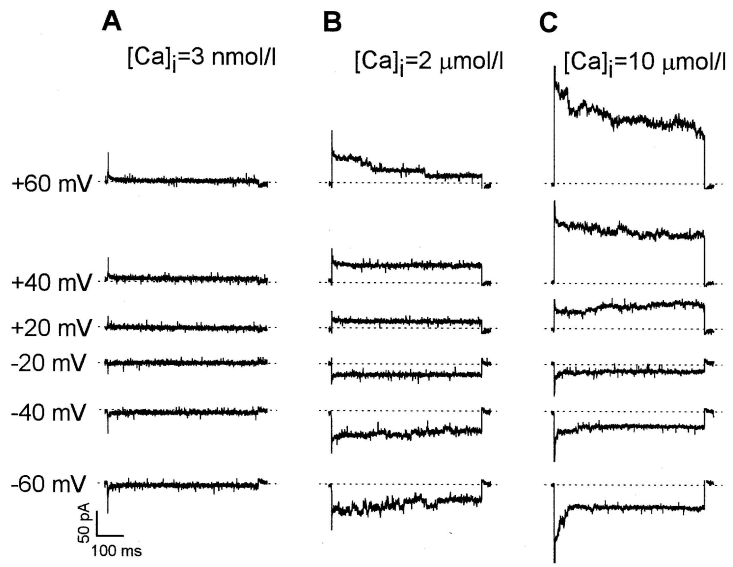

Figure 5. Large-conductance Cl^- current in whole-cell recordings in the presence of different intracellular Ca^{2+} concentrations. A) Current records elicited by voltage steps 600 ms-long (bath solution *Ext 1*, pipette solution *Int 1*). Membrane potentials relative to a holding potential of 0 mV are indicated at the *left* of each trace. Solid lines represent zero current levels. No Cl^- channel activity was detected ($n = 10$). B) Single or multiple Cl^- channels were seen in about 50 % of the experiments ($n = 24$) in the presence of 2 μmol/l intracellular Ca^{2+} concentration (pipette solution *Int 3*). C) Multiple Cl^- channels were observed in all whole-cell recordings in the presence of 10 μmol/l intracellular Ca^{2+} concentration ($n = 11$; pipette solution *Int 4*). Data filtered at 1 kHz.

−15 mV at negative values and 85 mV at positive values. In cell-attached patches that did not exhibit channel activity, exposure to a hypotonic bathing solution did not induce large-conductance anion currents (data not shown).

Ca^{2+}-dependence of the large-conductance anion channel in whole-cell recordings

Activity of large-conductance Cl^- channels could be recovered in most whole-cell recordings in the presence of 2 μmol/l or more intracellular Ca^{2+} concentrations. Single or multiple Cl^- channels were seen in about 50 % (12/24) of the experiments in the presence of 2 μmol/l Ca^{2+}, whereas 100% (11/11) of recordings displayed multiple Cl^- channels activity in the presence of 10 μmol/l Ca^{2+}. No channel activity was detected in the presence of 3 nmol/l Ca^{2+} ($n = 10$; see Fig. 5). In any case, the number of channels active in whole-cell was low compared to the number of channels active in excised patch. This raised the possibility that in physiological conditions the channels could be modulated by some intracellular factors in addition to Ca^{2+}.

Discussion

The results described here lend evidence for the presence of a large-conductance anion channel in N2A neuroblastoma cells. In excised patches, the biophysical characteristics of large-conductance Cl^- channel fell within those encountered in neuroblastoma cell lines (Falke and Misler 1989; Bettendorff et al. 1993; Forshaw et al. 1993) and in other cell membranes (Woll and Neumcke 1987; Pahapill and Schlichter 1992; Mitchell et al. 1997). Falke and Misler (1989) showed that hypotonic shock activates the anion channel in cell-attached conditions, and Bettendorff et al. (1993) reported that intracellular thiamine triphosphate concentrations turn the channel on without interfering with the voltage-dependent gating mechanism. In our preparation, the channel was frequently induced in excised patches by depolarising potentials (90%). In inside-out patches that did not exhibit channel activity, an elevation of intracellular Ca^{2+} neither induced single-channel currents nor affected the kinetics of channels subsequently activated by depolarising potentials. Channel activity was detected in 43 cell-attached patches, as compared with 96 patches eliciting channels only in subsequent excised patch configurations (31%). The channel was induced by extracellular application of the Ca^{2+}-ionophore A23187 in the presence of 0.2 μmol/l Ca^{2+} (80%) or 2 μmol/l Ca^{2+} (100%). The intracellular Ca^{2+} increase did not modify the duration of the channel active state before the inactivated state but the channel activity showed a flickering behaviour due to frequent transitions between the highest opening level and the baseline. Since periods of flickering were occasionally observed in excised patches, it could be suggested that the intracellular Ca^{2+}, through some unknown cytoplasmic factors, stabilises the kinetic states of the channel. Moreover, in whole-cell configuration, the anion channel activity was Ca^{2+}-induced, too, even though the number of channels activated by high intracellular Ca^{2+} concentrations was small, as compared with the probability to find channels in excised patches. This diversity suggests an indirect action of Ca^{2+} on the large-conductance anion channel, such as Ca^{2+}-dependent modifications to the channel by some other intracellular factors. In excised patches, the frequent detection of channels and the loss of Ca^{2+}-induction imply the removal of at least one such factor due to cell dialysis. Similar conclusion was drawn for the Ca^{2+}-dependence of anion channels in embryonic *Xenopus* spinal neurons (Hussy 1992). In other preparations, activation of Cl^- currents was found to be mediated by Ca^{2+}/calmodulin-dependent protein kinase (Nishimoto et al. 1991; Wagner et al. 1991). The diversity of Ca^{2+} entry pathways and mechanisms of their control in endothelial cells have been described by Nilius et al. (1998). An important observation resulting from the present study of neuroblastoma cells is that cell-attached recordings, unlike excised patches, show anion channels active in a wide range of membrane potentials and the maximal channel activity shifts towards more positive potentials. It is interesting to note that Hurňák and Zachar (1994) found changes in open probability between quiescent myoblasts and proliferating myoballs and a higher probability of incidence of large-conductance anion channels in cell-attached experiments in myoballs. The difference might be related to the

internal amino acid sequence of the channel being in contact with the cell interior in cell-attached patches. Similar asymmetrical behaviour has been described by Woll and Neumcke (1987), Pahapill and Schlichter (1992), and Kemp et al. (1993). In cell-attached patches showing single anion channel activity, the zero-current (reversal) potential was close to −10 mV as the resting potential of cells eliciting channel activity. A significant theory developed by Zambrowicz and Colombini (1993) and tested with the voltage-dependent anion channel (VDAC) found in the outer membrane of mitochondria, accounted rather well for the reversal potential of large-conductance channel current. These authors suggested that cations and anions can flow through large channels, and that multiple ions can be in the channel at the same time. The zero-current potential results in current flows in opposite directions. This might represent a common property of VDAC and large conductance anion channels. Dermietzel et al. (1994) suggested that a large conductance anion channel found in plasma membranes of astrocytes represents the VDAC channel. However, other aspects deserve consideration. The cell resting potential close to -10 mV in cells showing channel activity in the cell-attached mode should be compared to the resting potential close to −45 mV in cells in which no channel activity in the cell-attached mode was detected. This difference supports the hypothesis that the large-conductance Ca^{2+}-activated anion channel might play a role in the membrane potential modulation (Binggeli and Weinstein 1986; Arcangeli et al. 1995). Moreover, it was suggested that Ca^{2+}-dependent Cl^- channels might be involved in cell volume regulation and cell proliferation (Means 1994; Basavappa et al. 1995; Szücs et al. 1996; Nilius et al. 1997, 1998; Pedersen et al. 1998). In our cell-attached patches that did not exhibit channel activity, exposure to a hypotonic bathing solution did not induce large-conductance anion currents. As a consequence, given the fundamental importance of membrane depolarisation and Ca^{2+} regulation during the cell cycle, we suggest that the channel might contribute to cell proliferation in neuroblastoma cells.

Acknowledgements. This work was supported in part by CNR and in part by Linear Italia, Italy.

References

Arcangeli A., Bianchi L., Becchetti A., Favarelli L., Coronnello M., Mini E., Olivotto M., Wanke E. (1995): A novel inward-rectifying K^+ current with a cell-cycle dependence governs the resting potential of mammalian neuroblastoma cells. J. Physiol. (London) **489**, 455—471

Basavappa S., Chartouni V., Kirk K., Prpic V., Ellory J. C., Mangel A. W. (1995): Swelling-induced chloride currents in neuroblastoma cells are calcium dependent. J. Neurosci. **15**, 3662—3666

Becq F., Fanjul M., Mahieu I., Berger Z., Gola M., Hollande E. (1992): Anion channels in a human pancreatic cancer cell line (Capan-1) of ductal origin. Pflügers Arch. **420**, 46—53

Bettendorff L., Kolb H. A., Schoffeniels E. (1993): Thiamine triphosphate activates an anion channel of large unit conductance in neuroblastoma cells. J. Membrane Biol. **136**, 281—288

Binggeli R., Weinstein R. C. (1986): Membrane potentials and sodium channels: hypotheses for growth regulation and cancer formation based on changes in sodium channels and gap junction. J. Theor. Biol. **123**, 377—401

Dermietzel R., Hwang T. K., Buettner R., Hofer A., Dotzler E., Kremer M., Deutzmann R., Thinnes F. P., Fishman G. I., Spray D. C., Siemen D. (1994): Cloning and *in situ* localization of a brain-derived porin that constitutes a large-conductance anion channel in astrocytic plasma membranes. Proc. Natl. Acad. Sci. USA **91**, 499—503

Falke L. C., Misler S. (1989): Activity of ion channels during volume regulation by clonal N1E115 neuroblastoma cells. Proc. Natl. Acad. Sci. USA **86**, 3919—3923

Forshaw P. J., Lister T., Ray D. E. (1993): Inhibition of a neuronal voltage-dependent chloride channel by the type II pyrethroid, deltamethrin. Neuropharmacology **32**, 105—111

Franciolini F., Petris A. (1990): Chloride channels of biological membranes. Biochim. Biophys. Acta **1031**, 247—259

Geletyuk V. I., Kazachenko V. N. (1985): Single Cl^- channels in molluscan neurones: multiplicity of the conductance states. J. Membrane Biol. **86**, 9—15

Hurňák O., Zachar J. (1994): Conductance-voltage relations in large-conductance chloride channels in proliferating L6 myoblasts. Gen. Physiol. Biophys. **13**, 171—192

Hussy N. (1992): Calcium-activated chloride channels in cultured embryonic *Xenopus* spinal neurons. J. Neurophysiol. **68**, 2042—2050

Kajita H., Kotera T., Shirakata Y., Ueda S., Okuma M., Oda-Ohmae K., Takimoto M., Urade Y., Okada Y. (1995): A maxi Cl^- channel coupled to endothelin B receptors in the basolateral membrane of guinea-pig parietal cells. J. Physiol. (London) **488**, 65—75

Kawahara K., Takuwa N. (1991): Bombesin activates large-conductance chloride channels in Swiss 3T3 fibroblasts. Biochem. Biophys. Res. Commun. **177**, 292—298

Kemp P. J., MacGregor G. G., Olver R. E. (1993): G protein-regulated large-conductance chloride channels in freshly isolated fetal type II alveolar epithelial cells. Amer. J. Physiol. **265**, 322—329

Light D. B., Schwiebert E. M., Fejes-Toth G., Naray-Fejes-Toth A., Karlson K. H., McCann F. V., Stanton B. A. (1990): Chloride channels in the apical membrane of cortical collecting duct cells. Amer. J. Physiol. **258**, 273—280

Lindau M., Fernandez J. M. (1986): A patch-clamp study of histamine-secreting cells. J. Gen. Physiol. **88**, 349—368

Means A. R. (1994): Calcium, calmodulin and cell cycle regulation. FEBS Lett. **347**, 1—4

Mills J. W., Schwiebert E. M., Stanton B. A. (1994): The cytoskeleton and membrane tranport. Curr. Opin. Nephrol. Hypertens. **3**, 529—534

Mitchell C. H., Wang L., Jacob T. J. C. (1997): A large-conductance chloride channel in pigmented ciliary epithelial cells activated by GTPγS. J. Membrane Biol. **158**, 167—175

Nilius B., Prenen J., Voets T., Van den Bremt K., Eggermont J., Droogmans G. (1997): Kinetic and pharmacological properties of the calcium-activated chloride-current in macrovascular endothelial cells. Cell Calcium **22**, 53—63

Nilius B., Prenen J., Voets T., Eggermont J., Bruzik K. S., Shears S. B., Droogmans G. (1998): Inhibition by inositoltetrakisphosphates of calcium- and volume-activated Cl^- currents in macrovascular endothelial cells. Pflügers Arch. **435**, 637—644

Nishimoto I., Wagner J. A., Schulman H., Gardner P. (1991): Regulation of Cl^- channels by multifunctional CaM kinase. Neuron **6**, 547—555

Nobile M., Lagostena L. (1998): A discriminant block among K^+ channels types by phenytoin in neuroblastoma cells. Brit. J. Pharmacol. **124**, 1698—1702

Nobile M., Vercellino P. (1997): Inhibition of delayed rectifier K^+ channels by the anticonvulsant drug phenytoin. Brit. J. Pharmacol. **120**, 647—652

Pahapill P. A., Schlichter L. C. (1992): Cl^- channels in intact human T lymphocytes. J. Membrane Biol. **125**, 171—183

Pappas C. A., Ritchie J. M. (1998): Effect of specific ion channel blockers on cultured schwann cell proliferation. Glia **22**, 113—120

Pedersen S. F., Prenen J., Droogmans G., Hoffmann E. K., Nilius B. (1998): Separate swelling- and Ca^{2+}-activated anion currents in Ehrlich ascites tumor cells. J. Membrane Biol. **163**, 97—110

Robertson A. P., Martin R. J. (1996): Effects of pH on a high conductance Ca-dependent chloride channel: a patch-clamp study in *Ascaris suum*. Parasitology **113**, 191—198

Rouzaire-Dubois B., Dubois J. M. (1998): K^+ channel block-induced mammalian neuroblastoma cell swelling: a possible mechanism to influence proliferation. J. Physiol. (London) **510**, 93—102

Santella L. (1998): The role of calcium in the cell cycle: facts and hypotheses. Biochem. Biophys. Res. Commun. **244**, 317—324

Schlichter L. C., Sakellaropoulos G., Ballyk B., Pennefather P. S., Phipps D. J. (1996): Properties of K^+ and Cl^- channels and their involvement in proliferation of rat microglial cells. Glia **17**, 225—236

Schwiebert E. M., Karlson K. H., Friedman P. A., Dietl P., Spielman W. S., Stanton B. A. (1992): Adenosine regulates a chloride channel via protein kinase C and a G protein in a rabbit cortical collecting duct cell line. J. Clin. Invest. **89**, 834—841

Schwiebert E. M., Mills J. W., Stanton B. A. (1994): Actin-based cytoskeleton regulates a chloride channel and cell volume in a renal cortical collecting duct cell line. J. Biol. Chem. **269**, 7081—7089

Strange K., Emma F., Jackson P. S. (1996): Cellular and molecular physiology of volume-sensitive anion channels. Amer. J. Physiol. **39**, 711—730

Szücs G., Heinke S., Droogmans G., Nilius B. (1996): Activation of the volume-sensitive chloride current in vascular endothelial cells requires a permissive intracellular Ca^{2+} concentration. Pflügers Arch. **431**,467—469

Thorn P., Martin R. J. (1987): A high-conductance calcium-dependent chloride channel in *Ascaris suum* muscle. Quart. J. Exp. Physiol. **72**, 31—49

Vaca L., Kunze D. L. (1992): Anion and cation permeability of a large conductance anion channel in the T84 human colonic cell line. J. Membrane Biol. **130**, 241—249

Voets T., Szücs G., Droogmans G., Nilius B. (1995): Blockers of volume-activated Cl^- currents inhibit endothelial cell proliferation. Pflügers Arch. **431**, 132—134

Wagner J. A., Cozens A. L., Schulman H., Gruenert D. C., Stryer L., Gardner P. (1991): Activation of chloride channels in normal and cystic fibrosis airway epithelial cells by multifunctional calcium/calmodulin-dependent protein kinase. Nature **349**, 793—796

Woll K. H., Neumcke B. (1987): Conductance properties and voltage dependence of an anion channel in amphibian skeletal muscle. Pflügers Arch. **410**, 641—647

Wonderlin W. F., Strobl J. S. (1996): Potassium channels, proliferation and G1 progression. J. Membrane Biol. **154**, 91—107

Wu J. V., Shrager P. (1994): Resolving three types of chloride channels in demyelinated *Xenopus* axons. J. Neurosci. Res. **38**, 613—620

Young G. P. H., Young J. D. E., Deshpande A. K., Goldstein M., Koide S. S., Cohn Z. A. (1984): A Ca^{2+}-activated channel from *Xenopus laevis* oocyte membranes reconstituted into planar bilayers. Proc. Natl. Acad. Sci. USA **81**, 5155—5159

Zambrowicz E. B., Colombini M. (1993): Zero-current potentials in a large membrane channel: A simple theory accounts for complex behavior. Biophys. J. **65**, 1093—1100

Final version accepted March 16, 2000